



Seismic fragility analysis of LNG sub-plant accounting for component dynamic interaction

Muhammad Farhan¹ · Stathis Bousias¹

Received: 15 October 2019 / Accepted: 19 June 2020 / Published online: 25 June 2020
© Springer Nature B.V. 2020

Abstract

Earthquakes can cause significant damage to liquefied gas terminals, a critical part of lifeline facilities of energy supply networks, failure of which may lead to loss of hazardous material, explosion, environmental contamination, loss of functionality and disruption of business. To date, seismic risk analysis of such facilities mainly focuses at component level, with the inherent dynamic interaction between the supporting structure and non-structural components not receiving the merited attention. In the present study, the seismic performance of an actual facility comprising of a piping system and a reinforced concrete (RC) supporting structure is analyzed through a finite element model in the non-linear regime, both as coupled and decoupled case. Plastic strains are used as engineering demand parameters (EDP) to define leakage limit state for pipes. Since the RC pipe rack supporting structure is designed for low seismic loads, shear is recognized as the predominant failure mode. The same components are then analyzed in unison, considering coupling due to dynamic interaction. Fragility functions are estimated for both cases using multiple stripe analysis. A set of strong ground motions artificially generated using the specific barrier model, are employed for developing fragility curves. They are expressed with peak ground acceleration (PGA) as an intensity measure. Statistical estimation of the parameters of fragility functions are based on maximum likelihood method. It is inferred that in the decoupled case, pipes show higher vulnerability at lower PGA, at higher PGA pipe rack can fail suddenly resulting in total failure of the system. Moreover, in coupled case the fragility of the pipes and RC rack changes substantially because of the piping system boundary conditions. Thus, concluding that the risk estimation could be erroneous if dynamic interaction is neglected.

Keywords Fragility analysis · Dynamic interaction · Vulnerability analysis · Piping network · Supporting RC structure

✉ Muhammad Farhan
muhammadfarhan.nust@gmail.com

Stathis Bousias
sbousias@upatras.gr

¹ Department of Civil Engineering, University of Patras, 26504 Patras, Greece

1 Introduction

Fragility analysis is an important procedure for estimating seismic performance and overall risk associated with structures and industrial plants which is inherently related to the selected damage mechanisms both at local and system level. Fragility functions provide the probability of exceedance of a certain damage state over a range of ground motion intensities. Furthermore, they can be used for vulnerability studies to design different retrofitting schemes. The key parameters for performing the seismic fragility analysis are the input ground motions, selection of certain seismic intensity measure, selection of engineering demand parameter for each component, probabilistic demand analysis and method used for fragility estimation (Elnashai and Di Sarno 2015).

Like industrial infrastructures, refrigerated liquefied gas (RLG) terminals represent strategic infrastructures for energy supply with liquefied natural gas (LNG). They handle 10% of the global energy supply, via 29 LNG terminals along European coastline some of which are planned or being expanded due to increase in LNG imports EU (2018). Furthermore, ongoing European projects and future exploitation of natural resources will probably support exports to global markets and Europe via LNG or pipelines increasing the need for constructing more LNG terminals in the region. The main purpose of RLG is to store and distribute LNG, therefore, they play an important role in the energy cycle around the world and at regional levels. LNG terminals are necessarily constructed at coastal sites where a port is available for storage tanks and long transport infrastructure pertaining to both liquefaction and regasification (Fig. 1). The main process area includes pipe racks, knock-out drum (or vapor–liquid separator) and other process equipment. In liquefaction, the gas is liquified by compression and cooling to low temperature, whereas in regasification, the LNG is converted to its gaseous form for further distribution to the market.

Obviously, and similar to other industrial facilities, LNG plants carry a significant risk associated with natural hazards including fire and seismic events (Krausmann et al. 2009; Lanzano et al. 2015) as one or more pipeline failure/s may lead to a high-consequences' chain of events. The seismic potential is high in Central and East Mediterranean basin in which countries like Italy, Greece and Turkey have experienced severe catastrophic events during the last decades. In this respect, different case studies has been conducted to evaluate hazards (Baesi et al. 2013; Cozzani et al. 2014; Young et al. 2004). Complex methodologies in estimating the overall hazard e.g. Antonioni et al. (2007) and Campedel (2008) only partly consider the variability of seismic events and related domino effects.



Fig. 1 Overview of refrigerated liquefied gas (RLG) plant

A typical industrial plant consists of many structural and mechanical components (of steel mainly), including straight pipes, elbows, Tee-Joints, valves, flanged joints, pressure vessels, tanks, pipe racks, etc. Supporting structures or pipe racks carry complex systems of nonbuilding structures and nonstructural components that transfer hazardous substances from one unit to another, thus, their seismic integrity is critical as their failure may lead to leakage or eventual loss of containment (LOC) triggering fire, explosion or other type of environmental damage. While steel piping systems are usually quite flexible, supporting structures, specifically in existing RC ones are routinely designed to remain elastic under the design loads and less attention was paid to their response under intense seismic actions (Paolacci et al. 2015). Consequently, existing, non-seismically designed RC supporting structures may develop extensive damage due to lack of required capacity against seismic actions and can even fail before secondary systems (Kothari et al. 2017; Di Sarno and Karagiannakis 2019). Hence, when evaluating the risk of an existing LNG plant, fragility curves regarding the supporting structures are necessary.

To date, most of the research has focused on the investigation of the seismic response of critical components such as elbows, t-joints, bolted flange joints or simply by decoupling the response of the structure and the piping system. According to current design criteria (mainly originating from the nuclear industry) the interaction between two coupled vibrating components can be neglected should the mass of the interacting secondary component be lower than 1% of the supporting primary one (Fouquiau et al. 2018; Taghavi and Miranda 2008). Nevertheless, according to Firoozabad et al. (2015) if the secondary component is supported at multiple locations on the primary one and is rather extended, eventual coupled response effect should be investigated regardless of any mass percentage value. Fundamentally, if a decoupled analysis is to be carried out for a partial structure, it is vital to ensure that the decoupling does not significantly affect the frequencies and the response of the primary system.

The research is rather limited to undertake the dynamic interaction into account for both pipelines and pipe racks. There have been several European research projects completed such as STREST (Tsionis et al. 2016), Syner-G (Pitilakis et al. 2011) focusing on seismic hazard, vulnerability and risk of critical infrastructures. While in STREST the focus was mainly on developing methodologies for calculating risk of critical infrastructure systems under multiple-hazards, in Syner-G more attention was paid on fragility curves of individual equipment such as steel storage tanks, processing facilities and buried pipelines. Regarding the development of decoupled fragility curves, a simplified analysis is carried out without considering the coupled dynamic interaction by Firoozabad et al. (2015) for piping systems of nuclear power plants (NPP) and by Park and Lee (2015) for boil-off gas compressors at LNG terminals. An elbow and an anchor point (in former case) were identified as the critical section of the system and fragility curves are presented only for these critical components. Another study (Bursi et al. 2018) adopted the same decoupled fragility analysis for an LNG sub plant, in which an elbow was identified as a critical component and the risk against leakage was determined by developing the relevant fragility function. In a recent study by Salem et al. (2019) on seismic performance of pipe racks structures, fragility analysis was conducted on different pipe rack configurations—nevertheless, no dynamic interaction was considered to demonstrate a coupled analysis including pipelines.

The question remains, however, whether the dynamic interaction of pipe racks with pipelines or other supported components as a coupled system has, indeed, any noticeable effect on the response of these facilities and if, consequently, it should be considered for the risk assessment. This is particularly interesting in the case of industrial plants exhibiting simultaneous modes of component failure (pipelines and pipe rack for instance) that are

inherently coupled. This is the base and motivation of this research, investigating the fragility of components in decoupled and coupled case to find if the dynamic interaction plays an important role in risk assessment.

In this context the work presents seismic vulnerability assessment of an existing LNG sub-plant as a case study. The effort is to obtain fragility curves for the components of the sub-plant analyzed in decoupled and coupled state. The strong ground motions are selected from a database which were generated using specific barrier model (SBM) including basin effects, which plays an important role in response of industrial structures. Thus, after a brief review of existing fragility-curve evaluation methods, the definition of damage limit states and EDPs related to support structure and piping system, the seismic vulnerability is assessed using multiple stripe analysis (MSA) (Baker 2015). The related fragility parameters are estimated by using maximum likelihood method (MLM). Finally, comparison between the fragilities in coupled and decoupled case is presented by highlighting the importance of dynamic interaction for risk assessment.

2 Case study

The case study investigated in this research reproduces an existing LNG plant, the plan view of the plant is illustrated in Fig. 2. The main component of the plant is a 50 000 m³ ethylene storage tank that supplies LNG to the different process areas via stainless-steel piping system. Originally, according to the construction drawings, the sub-plant is designed for low seismicity; in stark contrast, to acquire additional information on the sub-plant performance for extreme lateral loadings, the components of horizontal pipe rack 1 (indicated with blue in Fig. 2) are examined for fragility analysis considering that the sub-plant is located in a high seismicity zone of Greece.

The piping system distributes ethylene from the base of the storage tank to different process areas, through horizontal pipe rack 1; the latter consists of two independent RC frame structures (“short” and “long” rack), shown in Fig. 3; the 9 m-long rack (“short”

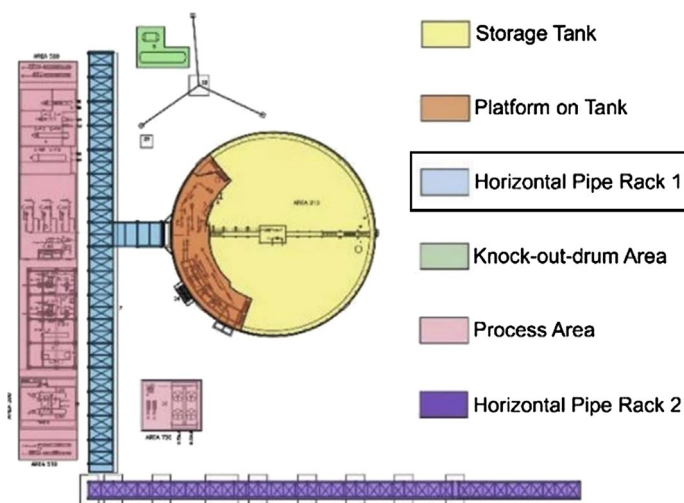


Fig. 2 Plan view of LNG plant with focus on Horizontal Pipe Rack 1

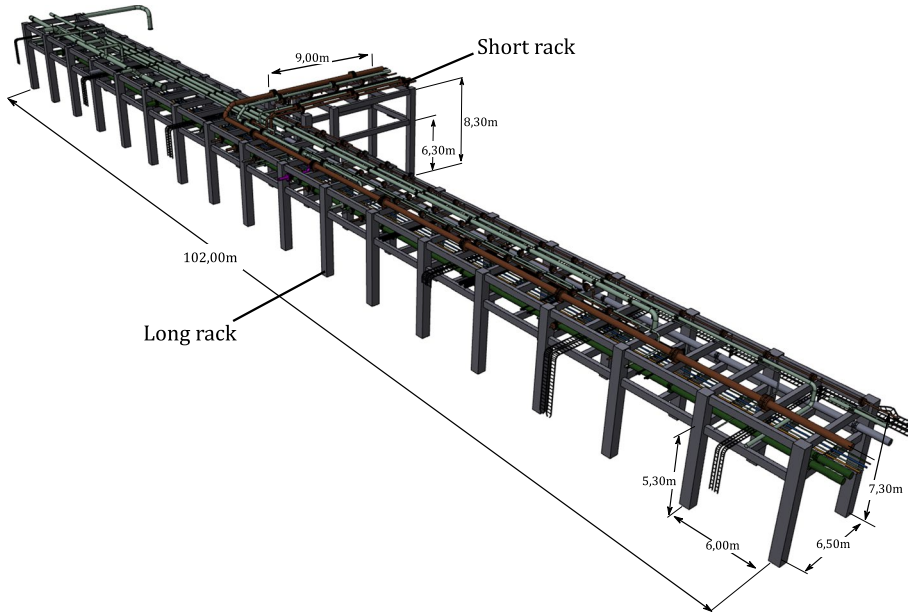


Fig. 3 Horizontal pipe rack 1 (short and long rack) under case study with numerous pipelines and other equipment's on top

rack) provides support to the pipelines running from the tank to the main (“long”) rack and is 6 m wide and 8.3 m high, with an intermediate level at 6.3 m above ground level. The rack is supported on four corner columns while transverse secondary beams are provided at 3 m spacing. Similarly, the 102 m-long rack (“long”) rack is perpendicular to the “short” one and is 6.5 m wide and 7.3 m high, also including an intermediate level at 5.3 m above ground level. Columns along the long dimension are 6 m apart, with transverse beams at roof level spaced every 3 m. Both RC racks are of concrete class C40/50.

While several pipelines of different diameters as well as other equipment are supported on the pipe racks as shown in Fig. 3, for the modelling purposes only the major (dimension-wise) pipelines connecting the RC rack to the storage tank are considered for the fragility analysis. The pipelines are welded and are made of stainless-steel grade ASTM A312/TP304L with different shapes and geometry arranged on horizontal pipe rack 1.

The LNG sub-plant has also been subject of research within the European research project INDUSE-2-SAFETY (Bursi and Reza 2016), focusing primarily on storage tank.

3 Numerical modelling of the case study

The numerical modelling of the case study considers two cases: in the first, components are treated and modelled individually (decoupled case), while in the second, racks and piping are considered as one system thus allowing consideration of the dynamic interaction between different components (coupled case).

3.1 Decoupled case

In the decoupled case, the study comprises both RC frames (short and long rack) and seven steel pipelines, each component being modelled separately and considering its own boundary conditions. Non-linear time history analysis is performed to obtain the behavior of each component. Results for fragility analysis for the decoupled case are discussed in Sect. 4.4.

3.1.1 Reinforced concrete frames

In order to perform seismic analysis, a finite element model (FEM) of the RC frame structure is established in the Seismostruct software (Seismosoft 2016). The beams in the RC racks are made up of 350 mm square section with four 20 mm-diameter rebars as longitudinal reinforcement of and 8 mm stirrups at 200 mm spacing for transverse. The 600 mm-side, square section columns comprised four 28 mm-diameter corner bars and two 25 mm-diameter intermediate bars per side, as well as 10 mm-diameter stirrups at 250 mm spacing (Fig. 4).

All RC elements are simulated via distributed-plasticity, fiber-discretized beam elements including geometric nonlinearity and material inelasticity. Each fiber is associated with a uniaxial stress–strain material relationship; the sectional stress state of the beam–column elements is then obtained through the integration of the nonlinear uniaxial stress–strain response of the individual fibers. Distributed inelasticity is attributed to columns and beams by using force-based elements, further sub-divided into seven Gauss–Lobatto integration sections for numerical integration. Different material constitutive laws are used for the RC cross section. The nonlinear model by Mander (Mander et al. 1988) is used for confined and unconfined concrete, whereas for the steel reinforcement the Menegotto–Pinto model (Menegotto and Pinto 1973) with isotropic hardening is employed. The parameters used for both constitutive models are given in Tables 1 and 2, respectively.

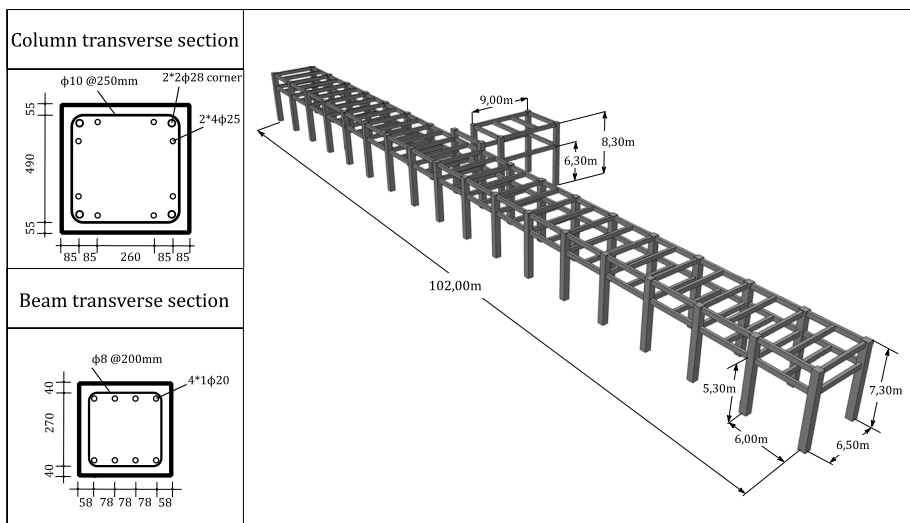


Fig. 4 RC pipe rack with transverse section of beam and column

Table 1 Parameters used for Menegotto–Pinto model for steel

Yield strength (f_y)	575 MPa
Elastic modulus (E)	210,000 MPa
Strain hardening parameter (b)	0.005
Transition curve initial shape parameter (R_0)	20
Transition curve shape calibrating coeff. (A1)	18.50
Transition curve shape calibrating coeff. (A2)	0.15

Table 2 Parameters used for Mander non-linear model for concrete

Mean compressive strength (f_c)	48 MPa
Mean tensile strength (f_t)	4.8 MPa
Elastic modulus (E)	35,220 MPa
Strain at peak stress (ϵ_{c0})	0.002

Table 3 Fundamental periods of the RC rack

Mode	Period (sec)	Modal mass (%)
1 (in shorter dimension “Y”)	0.250	59.98
5 (in longer dimension “X”)	0.218	97.11

Table 4 Pipeline cross sectional properties

Pipeline #	Diameter (mm)	Wall thickness (mm)	Curvature radius (mm)	Max pressure (bar)
1	406.40	7.92	610	2.8
2	273.05	4.19	381	0.2
3	114.30	3.05	152	0.2
4	168.28	3.40	229	0.0
5	323.85	4.57	457	0.3
6	219.08	3.76	305	16.3
7	168.28	3.40	229	1.0

The base of all columns in both RC racks is considered fixed. Loading from the pipes is transferred on the beams via their supports on the latter—uniform loading of 4 kN/m is additionally considered on the upper floor of each RC rack (e.g. pipes, cables, and electric installations). Result from modal analysis of the long RC rack in horizontal direction is included in Table 3.

3.1.2 Piping system

The piping system consists of seven main pipelines, which are modelled using FEM software ABAQUS (2016). The cross-sectional properties of each pipeline are summarized in Table 4.

The mechanical properties of the steel pipelines were determined through testing of metallographic samples of seamless pipes, per Bursi et al. (2018). Furthermore, to correctly model the steel constitutive law, the A312/TP304L stress–strain curve is reproduced with a bilinear relationship accounting for kinematic hardening, as shown in Fig. 5.

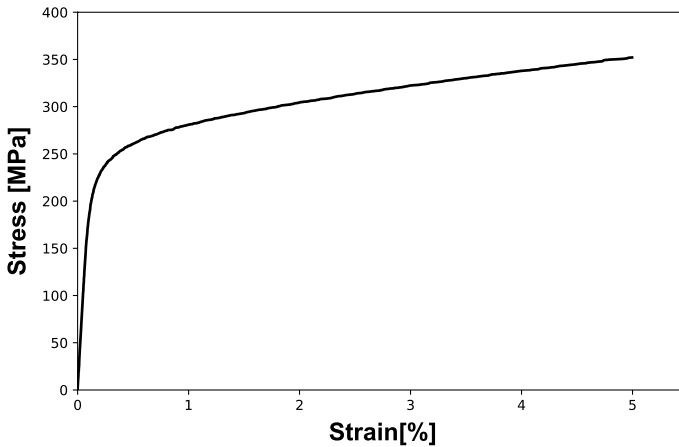


Fig. 5 Stress strain curve for steel pipelines A312/TP304L

All seven pipelines comprise different shapes and lengths, including elbows. Thus, to reasonably simulate the behavior of elbows including buckling and other phenomena, the finite continuum shell element (S4) is adopted for all pipelines. The S4 element in FEM includes four integration locations which makes it computationally more expensive. S4 elements can be used for problems prone to membrane- or bending-mode hour glassing, in areas where greater solution accuracy is required. Additionally, they can be used for problems where in-plane bending is expected. The selection of shell elements allows to directly account for pressure effects and ovalization on element flexibility (e.g. see Paolacci and Bursi 2014).

All seven pipelines are modelled and analyzed in Abaqus. For representation purposes they are shown together in Fig. 6, along with their respective boundary conditions. At their extremity on the storage tank pipelines are considered as pinned (represented with triangle in Fig. 6) with displacement being restrained in all three directions i.e. $U(X, Y, Z)$. At internal supports, where each pipeline is connected to reinforced concrete beams, two types of connections are considered, i.e. fixed or guided. Fixed supports (represented by a square) result in all movements being restrained in displacement $U(X, Y, Z)$ and rotation $UR(X, Y, Z)$. Relevant to the direction each pipeline runs on the RC racks, guided supports are utilized: displacements restrained in directions $U(X, Z)$ and denoted with a semi-circle, and displacements restrained in the direction $U(Y, Z)$, denoted by full circle.

For the analyses of the decoupled system the seismic excitation is applied at the internal supports i.e. fixed and guided, on the restrained directions for each pipeline, and the response is further analyzed for fragility analysis (see Sect. 4.4).

3.2 Coupled case

For the analyses of the coupled—a point that has received little attention in past studies—the whole system is modelled with all the components included and with their respective actual boundary conditions, considering the dynamic interaction between pipelines and pipe rack. The RC pipe rack supports are fixed at the ground level, while all seven pipelines are connected to the RC rack beams with the respective boundary conditions shown in Fig. 7. Due to increased number of degrees-of-freedom and

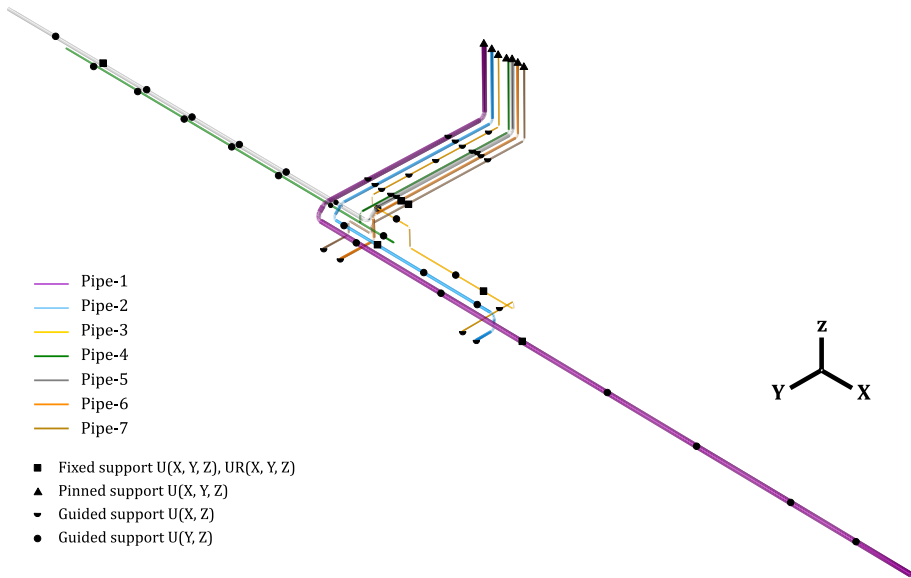


Fig. 6 Illustration of seven pipelines modelled in Abaqus with their respective boundary conditions

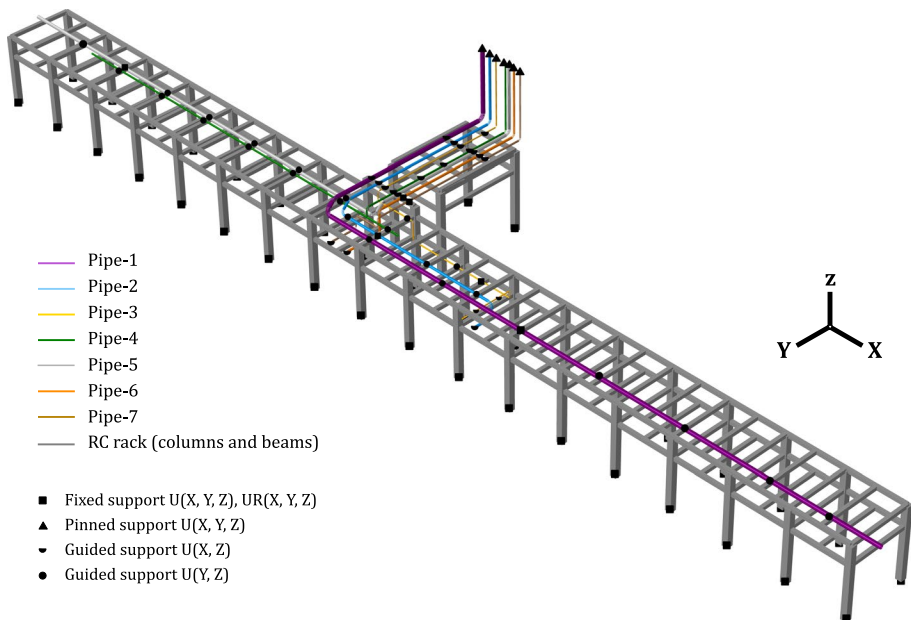


Fig. 7 Coupled case of the case study modelled in ABAQUS with respective boundary conditions

contact elements, the system becomes too complex and the detailed FEM analyses (as adopted in decoupled case) becomes an unrealistically cumbersome task; thus, “stick-type” elements are employed in the numerical model of the coupled case in the FE

Table 5 Comparison of RC rack eigen-periods of the coupled case with Midas and Abaqus

Direction	Midas period (s)	Abaqus period (s)	Difference (%)
Y	0.227	0.221	2.7
X	0.184	0.181	1.6

Table 6 Comparison of RC rack eigen-periods in coupled and uncoupled case

Direction	Uncoupled period (s)	Coupled period (s)	Difference (%)
Y	0.250	0.221	13
X	0.218	0.181	20

software ABAQUS (2016). The RC columns and beams of both racks are modelled with Timoshenko beam elements (B31H) which allow for transverse shear deformation and geometrical nonlinearity. Beams and columns are connected with rigid links- columns are considered fixed on the ground.

Pipelines comprise straight pipes and curved parts (elbows), connected through multi-point constraints (MPC). The straight parts of the pipes are modelled by means of PIPE31 elements, while elbows are modelled using special elbow elements (ELBOW31). In the latter, ovalization of pipe wall is made continuous from one element to the next, thus considering the interaction between elbows and adjacent straight segments of the pipeline. Same modeling strategy is employed for the components as in decoupled case. As discussed in Sect. 3.1.2, two types of constraints are applied in modelling the contact between piping system and RC support structure: (i) fixed constraint on beams of RC rack where movement is restrained both in displacement and rotation, (ii) roller or sliding support, allowing the pipe to slide in its longitudinal direction. Coupling of kinematic type is introduced at the points of support of pipes on beams, achieved via restraining relative displacement and/or rotation (as per construction drawings). The complete FE model is shown in Fig. 7, with a total of 6244 B31H elements, 3108 PIPE31 elements and 2955 ELBOW31 elements.

Seismic excitation is applied directly on the fixed supports of the RC rack at the ground level and the response is recorded for each component of the case study for fragility analysis (see Sect. 4.5). Another similar model was developed in Midas GEN (2018), in order to compare the modal response of the RC rack for the fully coupled case. In this model, straight pipe parts are modelled by beam linear elements and elbows with shell elements, with rigid links connecting them. To model columns and beams of the support structure, beam elements were employed. The constraints in representing boundary conditions between the pipelines and the structure were identical to the ones in Abaqus. The comparison of results from the modal analysis is provided in Table 5.

The results from the modal analysis of both models show satisfactory agreement—ABAQUS was used in the sequel for the fragility analysis. Comparison of modal analysis results as shown in Table 6 for the RC racks in the decoupled and the coupled cases reveals that the presence of pipelines and their support on the RC beams, lead to a stiffer response for the racks, along both directions.

4 Seismic vulnerability assessment of LNG sub-plant

Seismic vulnerability of existing industrial plants requires careful assessment and fragility analysis has been used for this purpose. The methodology used to perform entire procedure is schematically illustrated in Fig. 8.

In the following, the steps taken to perform fragility analysis are presented and discussed. In particular, the discussion is based on selection of seismic input, selection of EDP, probabilistic seismic analysis and fragility assessment method for the fragility curve estimation.

4.1 Selection of seismic input

For time-history analysis, seismic loading is defined by given ground motion variation in time. In principle, an adequate number of ground motions must be selected for the seismic analysis, forming an unbiased sample that can represent seismic hazard and seismotectonics at the site of interest. For the purpose of this study though, broader bins of ground motions including basin effects are selected, as provided by project RASOR (Papadrakakis et al. 2015).

It is generally accepted that seismic body waves striking geological formations in the form of basin deposits generate surface waves (Rayleigh and/or Love), with the latter leading to considerable lengthening of the duration of the seismic shaking and with concurrent increase on the spectral amplitudes for long periods (thus, particularly affecting the types of structures encountered in industrial plants). To include these effects in the seismic motions to be employed in the subsequent analysis one can generate strong motion records for basins by scaling up low level seismic records from basins. This is achieved via the convolution of the low-level seismic records with an appropriate “noise filter”, with parallel amplification of the spectral amplitudes (Papadrakakis et al. 2015). To that end, a set of 150 records has been generated using Stochastic modeling approach (SMA) with ground motion prediction equation (GMPE) and magnitude set within the range of $5.5 < M_w < 7.0$. Both near-and-far field records are used, distinguished on a threshold source-to-site distance (R_{jb}) between 10 to 150 km. Suites of synthetic earthquake strong ground motions (SGM) were generated using Rock B and soil type C and D, with random basin generated surface waves (BGSW) parameters. The “Specific Barrier model” (SBM) and its scaling law have been employed, as calibrated by (Papageorgiou 2003) for earthquakes

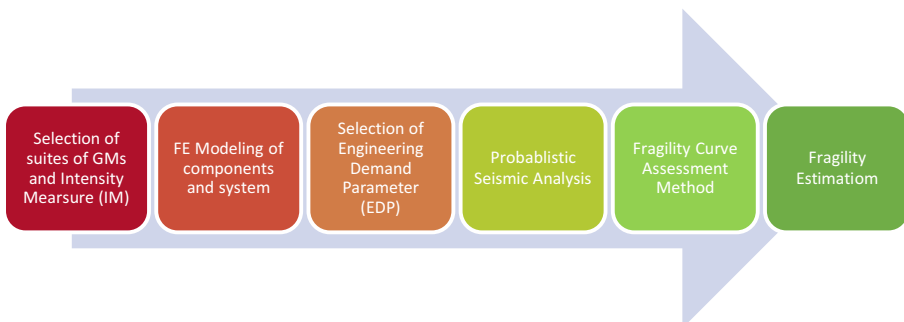


Fig. 8 Flow-chart for the fragility analysis

Fig. 9 Response Spectra of un-scaled records

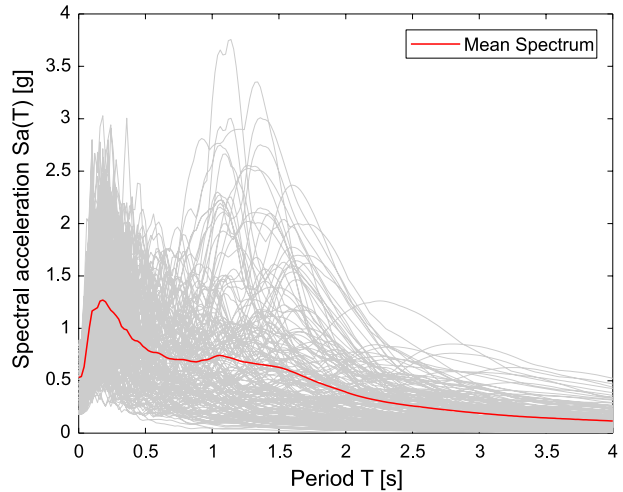


Table 7 Performance levels given in Vathi et al. (2017)

Level	Description
0	No damage
I	Minor (non-severe) damage
II	Major damage, but no loss of containment
III	Major damage with loss of containment

at extensional tectonic regions. It has been shown (Papadrakakis et al. 2015) that the so-obtained source spectrum compares well to that of actual strong motion records in Greece (Margaris and Hatzidimitriou 2002). The response spectrum of all un-scaled records with the mean spectrum is shown in Fig. 9.

4.2 Selection of engineering demand parameters

Probabilistic seismic demand analysis is used to determine the response of structures from the selected ground motions as part of seismic vulnerability assessment. This can be performed adopting different EDPs consistent with the damage states expected in each component of the sub-plant under study. Particular attention should be paid on the collapse limit state of the RC rack, as it can trigger failure of the sub-plant by influencing other secondary structures, like pipelines supported on it. Similarly, for pipes and elbows leakage conditions are considered because of the possibility of LOC and dispersion of dangerous materials (LNG in this case).

4.2.1 Performance of pipelines

To investigate the leakage condition triggered by seismic action on pipelines, attention is paid on the identification of reliable EDPs related to leakage limit state. In the literature, the performance of pipelines is mainly related to strain limits. To classify the performance of elbows, Vathi et al. (2017) defined the four levels of damage given in Table 7.

Depending on the performance level set of a pipe, the failure modes considered are those of local buckling and failure in tension. The performance level of interest in this study is LOC or collapse limit state, which correspond to damage level III. The failure modes, the relevant EDPs and the related limit states associated with each performance level, are summarized in Table 8.

In the Table, ϵ_Y is the yield strain of pipes (see Fig. 5) and ϵ_{Cu} is the critical compressive strain per Vathi et al. (2017):

$$\epsilon_{Cu} = 0.5\left(\frac{t}{D}\right) - 0.0025 + 3000\left(\frac{\sigma_h}{E}\right)^2 \tag{1}$$

with t denoting the thickness of the pipe walls, D the diameter, σ_h the hoop stress due to internal pressure and E the elastic modulus. Critical compressive strains for damage level III are for each pipeline calculated accordingly via Eq. (1) and utilizing values from Table 4. The resulting compressive strain values for the seven pipelines are 3.6%, 2.5%, 5.4%, 3.8%, 2.2%, 4.7% and 3.8%, respectively. These values of compressive strains are significantly higher than the leakage tensile strain pertaining to damage level III suggested by Vathi et al. (2017), i.e. 2% for major damage with loss of containment, thus allowing to consider tensile strain as the critical indicator of leakage and EDP for fragility analysis. This also complies to the extensive experimental work of Karamanos (2016) and the test campaign conducted by the Japan Nuclear Energy Safety Organization and the Nuclear Power Engineering Corporation of Japan (DeGrassi et al. 2008). In agreement with the experiments and test campaigns, we assume that piping experiences leakage conditions when tensile strain of about 2% develops on its outer surface.

4.2.2 EDP for RC frames

Vulnerability assessment of existing RC structures in industrial plants is of high significance because these are not usually seismically designed—should they fail, domino effects can be triggered in LNG plants. Concerning RC structural members, two failure modes are identified i.e. flexural (ductile) and failure in shear (brittle) according to Annex A of EN 1998–3 (2004) and three limit states are defined as per Table 9 along with relevant guidelines for the assessment of existing RC structures on the basis of the identified failure mode.

Table 8 Acceptance criteria for steel pipelines (adopted from Vathi et al. 2017)

Failure mode	Engineering demand parameter	Performance level and corresponding range	
Tensile fracture	Tensile strain $\epsilon_T(\%)$	$\epsilon_T \leq \epsilon_Y$	0
		$\epsilon_Y < \epsilon_T \leq 0.5\%$	I
		$0.5\% < \epsilon_T \leq 2\%$	II
		$\epsilon_T \geq 2\%$	III
Local buckling	Compressive strain $\epsilon_C(\%)$	$\epsilon_C \leq \epsilon_Y$	0
		$\epsilon_Y < \epsilon_C \leq \epsilon_{Cu}$	I
		$\epsilon_{Cu} < \epsilon_C \leq 5\epsilon_{Cu}$	II
		$\epsilon_C \geq 5\epsilon_{Cu}$	III

Table 9 Acceptance criteria for concrete members (Adapted from Fardis (2014))

Failure mode	Damage limitation (DL)	Significant damage (SD)	Near collapse (NC)
Flexure (rad)	$\theta_E \leq \theta_y$	$\theta_E \leq 0.75\theta_{u,m-\sigma}$	$\theta_E \leq \theta_{u,m-\sigma}$
Shear (kN)	$V_E \leq V_{Rd,EC2}$	$V_E \leq 0.75V_{Rd,EC8}$	$V_E \leq V_{Rd,EC8}$

In the Table, θ_E denotes the chord rotation demand from the analysis, θ_y the chord rotation at yielding, $\theta_{u,m-\sigma}$ is the mean-minus-standard deviation chord-rotation, V_E is the shear force demand from analysis, $V_{Rd,EC2}$ is the shear resistance before flexural yielding for monotonic loading per Eurocode 2 and $V_{Rd,EC8}$ is the cyclic shear resistance of the plastic hinges after flexural yielding per EN 1998–3 (2004). The main interest is again Near-Collapse (NC) limit state, thus for both failure modes NC limit state is used for analysis.

Preliminary analysis of RC rack of the case study conducted with Seismostruct (Seismosoft 2016) revealed that beams and columns failed in shear before their flexural capacity is attained. This behavior results from the initial design of the RC rack, as has been observed by Tsionis and Fardis (2014) for existing structures. For shear failure mode, the capacity ($V_{Rd,EC8}$) at Near Collapse limit state in Table 9 is estimated per EN 1998–3, Annex A (2004) as:

$$V_R = \frac{1}{\gamma_{el}} \left[\frac{h-x}{2L_v} \min(N; 0.55A_c f_c) + \left(1 - 0.05 \min\left(5; \mu_{\Delta}^{pl}\right) \right) \cdot \left[0.16 \max(0.5; 100\rho_{tot}) \left(1 - 0.16 \min\left(5; \frac{L_v}{h}\right) \right) \sqrt{f_c} A_c + V_w \right] \right] \tag{2}$$

where γ_{el} is the partial factor for seismic elements (1.5 for primary seismic elements), h is the depth of cross section, x is the compressive zone depth, N is the compressive axial force, μ_{Δ}^{pl} is the plastic part of ductility demand (calculated as the ratio the plastic part of the chord rotation, θ , normalized to the chord rotation at yielding, θ_y , determined per A-3.1.1 and per A-3.1.3 of EN-1998–3, respectively), shear span L_v is the ratio moment/shear at the end section, A_c is the cross sectional area, f_c is the concrete compressive strength, ρ_{tot} is the total longitudinal reinforcement ratio and $V_w = \rho_w b_w z f_{yw}$ the contribution of transverse reinforcement to shear resistance. As a result, shear capacity was selected as the EDP in fragility analysis for the RC frames.

4.3 Fragility assessment method

Structural fragility, defined as the conditional probability of exceeding a certain damage state or collapse, for a given intensity measure, is (Baker 2015):

$$P(C|IM = x) = \Phi\left(\frac{\ln(x/\theta)}{\beta}\right) \tag{3}$$

where $P(C|IM = x)$ is the probability that a ground motion with intensity measure $IM = x$ will cause structural failure or exceedance of certain limit state, $\Phi(\cdot)$ is the standard normal cumulative distribution function (CDF), θ is the median of the intensity measure (IM) and β is the standard deviation. Cloud method (Cornell et al. 2002), incremental dynamic analysis (IDA) (Vamvatsikos and Cornell 2004) and multiple-stripe analysis (MSA) (Jalayer and Cornell 2009) are the most common methods for deriving fragility functions. Both

IDA and MSA are suitable for evaluating the relationship between EDP and IM, for a wide range of IM values; however, their application is time consuming as repetitive nonlinear dynamic analyses have to be performed over a wide range of increasing IM levels. In literature, most of the work is done by selecting handsome amount of natural accelerograms and performing simplified analysis e.g. linear regression analysis to compute the parameters for fragility functions (Bursi et al. 2018; Caprinuzzi et al. 2017; Paolacci et al. 2018).

In, incremental dynamic analysis ground motions are incrementally scaled to obtain structural response at increasing levels of the IM, which may result in scaling up to impractical IM levels. When MSA is employed, analyses are performed at discrete sets of IM levels, with and site-specific ground motions at different IM levels being chosen. It is currently considered preferable to choose representative GM’s at each intensity level, rather than taking handsome amount of GM’s and scaling them across all intensities—compared to IDA, the MSA may not yield increasing fractions of collapse with increasing IM. In this study, MSA is selected, not only because a GM database with a wide range of IM levels is available, but also the method is more efficient compared to IDA and cloud method (Baker 2015). The appropriate fitting technique for this type of analysis is to use method of maximum likelihood (Straub and Der Kiureghian 2008).

At each intensity level $IM = x_j$, a number of collapses are identified via structural analyses for a number of ground motions. Assuming that occurrence of collapse due to a ground motion is independent of the results for other ground motions, the probability of observing z_j collapses out of n_j ground motions with $IM = x_j$ is given by the binomial distribution.

$$P = \binom{n_j}{z_j} p_j^{z_j} (1 - p_j)^{n_j - z_j} \tag{4}$$

wherein p_j is the probability that a ground motion with $IM = x_j$ will cause collapse. The goal is to identify the fragility function that can predict p_j ; the maximum likelihood approach identifies the fragility function that gives the highest probability of collapse from the observed data, obtained from structural analysis. Analyses data is obtained at multiple IM levels, by taking the product of the binomial probabilities (Eq. 4) at each IM level to yield the likelihood for the entire data set:

$$Likelihood = \prod_{j=1}^m \left(\binom{n_j}{z_j} p_j^{z_j} (1 - p_j)^{n_j - z_j} \right) \tag{5}$$

where m is the number of IM levels. Using Eq. (3) for p_j , the fragility parameters become explicit in the likelihood function.

$$Likelihood = \prod_{j=1}^m \left(\binom{n_j}{z_j} \Phi \left(\frac{\ln(x_j/\theta)}{\beta} \right)^{z_j} \left(1 - \Phi \left(\frac{\ln(x_j/\theta)}{\beta} \right) \right)^{n_j - z_j} \right) \tag{6}$$

Estimates of fragility function parameters are obtained by maximizing this likelihood function:

$$\{\theta', \beta'\} = \arg \max \sum_{j=1}^m \left\{ \ln \binom{n_j}{z_j} + z_j \ln \Phi \left(\frac{\ln(x_j/\theta)}{\beta} \right) + (n_j - z_j) \ln \left(1 - \Phi \left(\frac{\ln(x_j/\theta)}{\beta} \right) \right) \right\} \tag{7}$$

4.4 Inelastic seismic analysis in decoupled case

Non-linear dynamic time history analysis is performed for all major components of sub-plant discussed in Sects. 3.1.1 and 3.1.2. Fragility parameters are estimated, via MSA and MLM. The generated ground motions (see Sect. 4.1) are sorted for each IM level (increment of 0.1 g) for levels increasing from 0 to 1 g, consequently selecting 15 records for each IM level in total of 10 levels.

In case of RC racks, a series of nonlinear time history analyses are performed at each IM level. A total of 150 simulations are carried out for the RC racks, applying the GMs in all 3 direction, with the strongest component being applied along X-axis, the main horizontal direction of the structure. Shear force demands (selected as an EDP) are recorded at each time step and compared to the member capacity (Eq. 2) of the respective members. Simulation results showed that columns failed prematurely in shear, with the beams to follow.

Concerning the piping system, a nonlinear dynamic analysis is performed for each pipe, including the effect of internal pressure. Equal number of simulations are carried out for each pipe, with tensile strains being recorded as EDP. Tensile strains were identified to accumulate mostly in elbows and fixed supports of the pipelines. The fragility curves developed for the decoupled case, according to assessment method set forth earlier, are shown in Fig. 10 (their parameters are included in Table 10).

From Fig. 10, depicting the results for fragility analysis of the components in decoupled case, it is observed that pipes seem to fail prior to the RC rack, exhibiting notable vulnerability at low PGA. Columns and beams of the RC racks exhibit sudden failure due to the brittle nature of the governing failure mode.

4.5 Inelastic seismic analysis in coupled case

The analysis of the complete system under study (coupled system—see Sect. 3.2) comprises static and dynamic analysis phases (Fig. 11). The static analysis is performed to consider internal pressure, gravity and dead loads, while the dynamic analysis is performed to account for the results coming from static step and applying seismic loading.

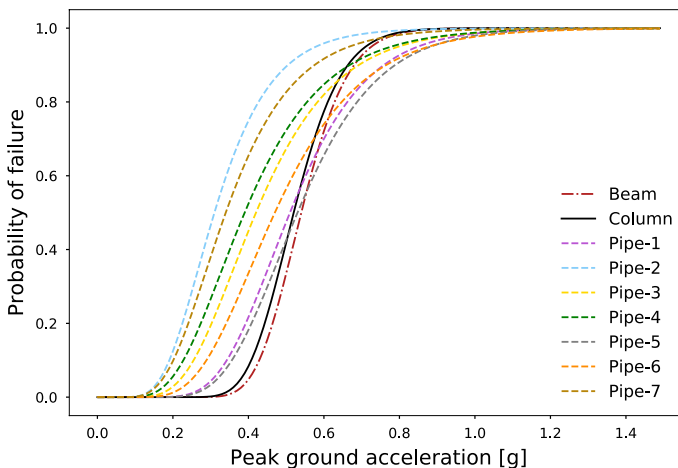
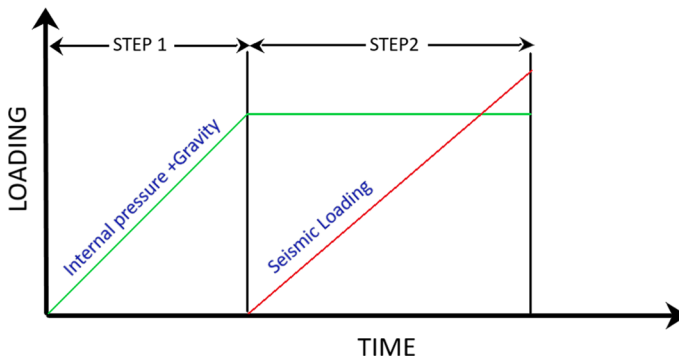


Fig. 10 Component fragility curves for decoupled case

Table 10 Fragility function parameter—decoupled case

Component	Parameters	
	$\theta'(g)$	β'
Pipe1	0.51	0.31
Pipe2	0.31	0.38
Pipe3	0.42	0.39
Pipe4	0.39	0.42
Pipe5	0.53	0.31
Pipe6	0.47	0.38
Pipe7	0.34	0.41
Column	0.52	0.19
Beam	0.54	0.18

**Fig. 11** Loading procedure for inelastic seismic analysis in coupled case

As done for the decoupled system components, 150 simulations are performed for coupled case with same records in each IM level. Same EDP's are recorded for the components in the coupled case i.e. shear for the RC members of the supporting rack and tensile strains for all pipelines. The fragility curves developed for the coupled case are illustrated in Fig. 12, whilst their parameters are listed in Table 11.

For the coupled system, dynamic interaction led to the components showing lower vulnerability compared to the decoupled case, with the only exception being the beams, which presented high vulnerability due to the increased shear forces experienced at the points of pipe supports. As a result, this behavior can trigger a major LOC event leading to domino effects. Furthermore, it can be observed that the steepness of the fragility curve of the pipes reduces substantially due to the coupling effect.

4.6 Component fragility comparison for coupled and decoupled scenarios

The fragility curves determined for the components of LNG sub-plant (RC frames and seven pipelines) considered as decoupled and coupled cases are presented in Fig. 13 (for the RC frames) and Fig. 14 (for pipelines). As far as the RC frames are considered, the columns of the RC rack showed higher vulnerability in the decoupled case (Fig. 13), whereas

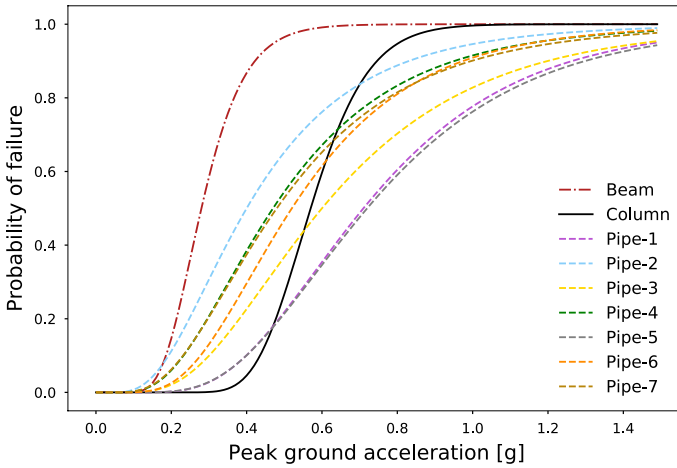


Fig. 12 Component fragility curves for coupled case

Table 11 Fragility function parameters—coupled case

Component	Parameters	
	$\theta'(g)$	β'
Pipe1	0.71	0.45
Pipe2	0.4	0.57
Pipe3	0.6	0.54
Pipe4	0.47	0.55
Pipe5	0.72	0.46
Pipe6	0.52	0.49
Pipe7	0.48	0.57
Columns	0.57	0.21
Beams	0.28	0.32

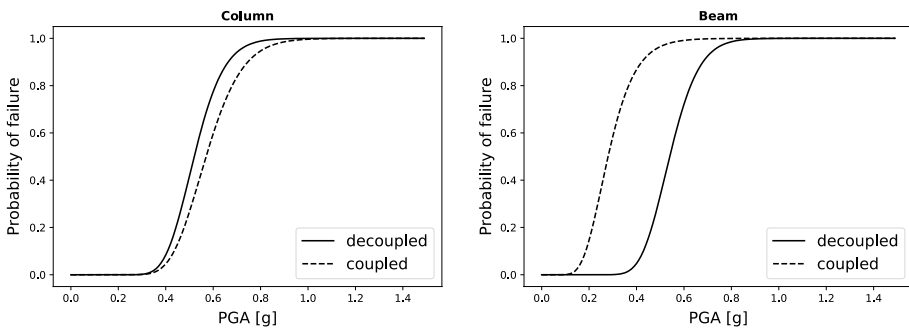


Fig. 13 Comparison of fragility curves of columns and beams between coupled and decoupled case

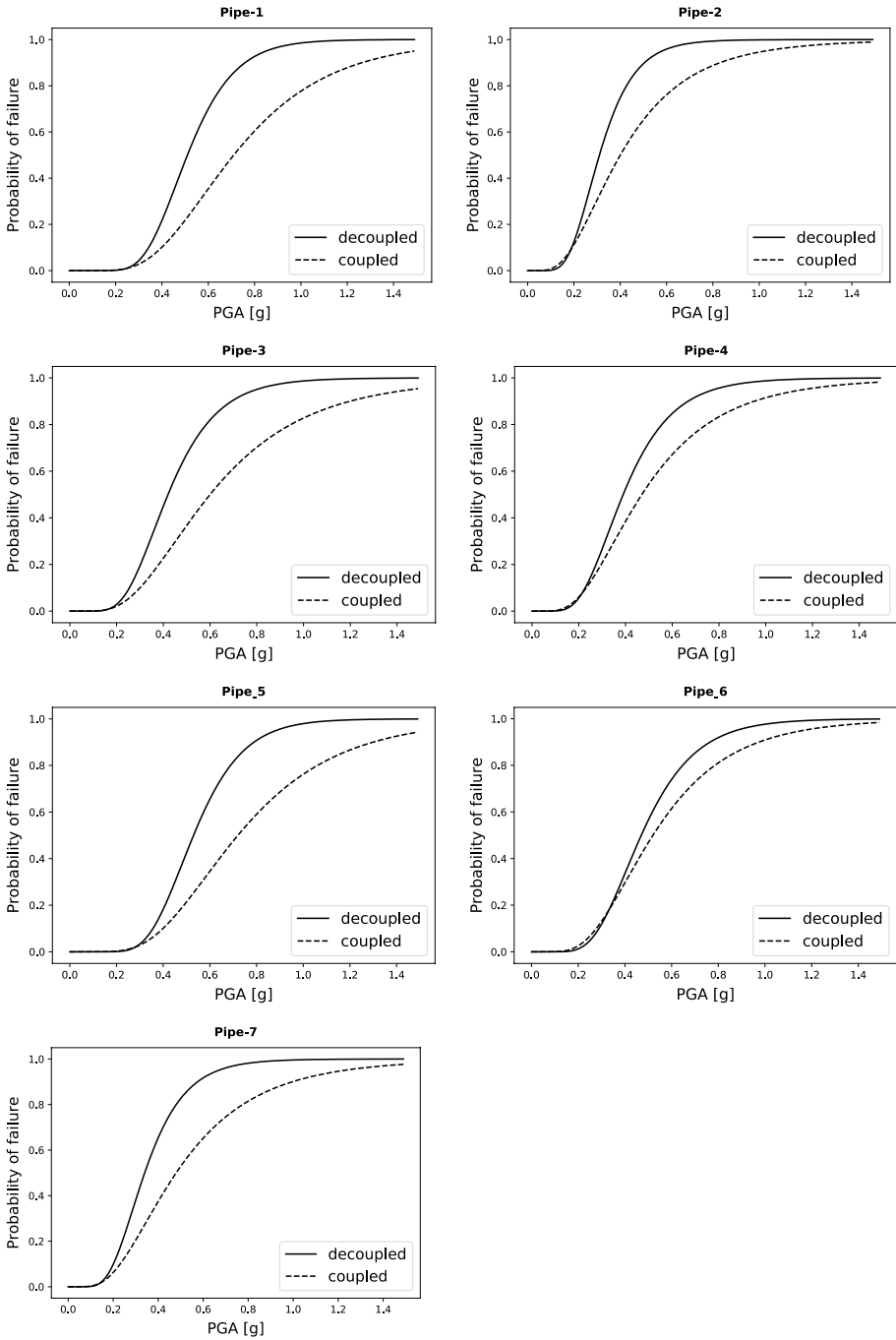


Fig. 14 Comparison of fragility curves of pipelines between coupled and decoupled case

in the coupled case the probability of failure decreases by 20% (e.g. at 0.5 g PGA level columns had 46% failure probability in decoupled case while in coupled case failure probability decreases to 25%), the reason being that, in the presence of pipelines and their boundary conditions, columns experience lower drift demands in the coupled case. In case of beams, the situation is markedly different e.g. at 0.5 g beams had 35% failure probability in decoupled case, with the probability of failure increasing up to 98% in the coupled case. This behavior is an outcome of the shortage of beam capacity in shear to face the demand resulting from the presence of the pipe supports over them.

As far as pipelines are concerned, their performance is comparatively similar with the case of RC rack, as failure probability drops by approximately 20–30% between the decoupled and the coupled case, with the steepness of the fragility curve being significantly reduced, as shown in Fig. 14. Furthermore, pipelines result highly vulnerable to LOC when considered as individual components (decoupled case) because of the application of GM's directly on the supports—their response significantly decreases when dynamic interaction is considered, because they experience lower displacements at beam level. It should be noted that vulnerability of pipelines is influenced by a number of factors i.e. shape of the pipe, boundary conditions and support type on the RC rack—due to these governing factors pipes 1, 3, 5, and 7 are affected more by dynamic interaction (coupled case) than pipes 2, 4, and 6. Consequently, the approach of decoupling the response of structural and non-structural components striving to simplify the assessment process, could overlook important aspects and overestimate or underestimate the seismic response of the components.

5 Conclusions

The effects of dynamic interaction between different components of an LNG sub-plant on seismic fragility curves are investigated in this paper, to cover the relevant gap in technical literature. A case study of an existing LNG sub-plant was selected, comprising reinforced concrete frame structures and an appreciable number of pipelines supported on them. Appropriate strong ground motion records at different intensity levels were generated using stochastic modeling and ground motion prediction equation, to be employed in the subsequent fragility analysis. The components of the sub-plant were treated both individually (decoupled case) and as interacting elements (coupled case).

The main findings of this research on a case study of an industrial plant may be summarized as follows:

- When coupled response of system components' is considered drift demand on the RC rack is reduced due to the presence of pipelines via their respective support conditions on the beams of the frame.
- For almost all components of the system examined higher vulnerability is noted when the components are considered as decoupled rather than in the opposite case.
- RC rack beam elements being an exception to the above showed very high vulnerability in the case dynamic interaction among plant components is considered—their vulnerability in the case examined increased up to 50% in coupled case owing to the loading exerted on them by the pipelines at their supporting points.
- In case of columns, vulnerability decreases by 20% in coupled case, due to the increase in the stiffness of the system when pipelines are incorporated in the analysis.

- Same behavior is observed in case of pipelines that the coupled system decreased the vulnerability by 20–30%.

The results show that the approach in which, for reasons of computational economy and simplification of the assessment process, no interaction among system's components response is considered, may yield misleading results in decision making. Taking into account that the assessment of LNG plants should be commensurate to their cruciality, system component interaction should be considered in order to avoid misleading risk estimation. Furthermore, accounting for dynamic interaction can help in identifying possible changes (e.g. boundary conditions/constraints at pipeline supports) such that may lead to improved system response.

Acknowledgements The support European Commission's Framework Program "Horizon 2020" to the first author, through the Marie Skłodowska-Curie Innovative Training Networks (ITN), XP-Resilience project (Grant Agreement No 721816), is greatly acknowledged.

References

- ABAQUS® (2016) ABAQUS- Dassault Systèmes® 3D Software. <https://www.simuleon.com/simulia-abaqus>
- Antonioni G, Spadoni G, Cozzani V (2007) A methodology for the quantitative risk assessment of major accidents triggered by seismic events. *J Hazard Mater* 147(1–2):48–59. <https://doi.org/10.1016/j.jhazmat.2006.12.043>
- Baesi S, Abdolhamidzadeh B, Hassan CRC, Hamid MD, Reniers G (2013) Application of a multi-plant QRA: a case study investigating the risk impact of the construction of a new plant on an existing chemical plant's risk levels. *J Loss Prev Process Ind* 26(5):895–903. <https://doi.org/10.1016/j.jlp.2012.11.005>
- Baker JW (2015) Efficient analytical fragility function fitting using dynamic structural analysis. *Earthq Spectra* 31(1):579–599
- Bursi OS, di Filippo R, La Salandra V, Pedot M, Reza MS (2018) Probabilistic seismic analysis of an LNG subplant. *J Loss Prev Process Ind* 53:45–60. <https://doi.org/10.1016/j.jlp.2017.10.009>
- Bursi OS, Reza MS (2016) Component fragility evaluation, seismic safety assessment and design of petrochemical plants under design-basis and beyond-design-basis accident conditions. In: Mid-Term Report, INDUSE-2-project, Contr. No: RFS-PR-13056, Research Fund for Coal and Steel SAFETY Project
- Campedel M (2008) Analysis of major industrial accidents triggered by natural events reported in the principal available chemical accident databases. JRC scientific and technical reports, <https://publications.jrc.ec.europa.eu/repository/handle/111111111/10929>
- Caprinuzzi S, Ahmed M, PaolacciBursiLa Salandra FOSV (2017) Univariate fragility models for seismic vulnerability assessment. *Press Vessels Pip Conf*. <https://doi.org/10.1115/PVP2017-65138>
- Cornell CA, Jalayer F, Hamburger RO, Foutch DA (2002) Probabilistic basis for 2000 SAC federal emergency management agency steel moment frame guidelines. *J Struct Eng* 128(4):526–533. [https://doi.org/10.1061/\(ASCE\)0733-9445\(2002\)128:4\(526\)](https://doi.org/10.1061/(ASCE)0733-9445(2002)128:4(526))
- Cozzani V, Antonioni G, Landucci G, Tugnoli A, Bonvicini S, Spadoni G (2014) Quantitative assessment of domino and NaTech scenarios in complex industrial areas. *J Loss Prev Process Ind* 28:10–22. <https://doi.org/10.1016/j.jlp.2013.07.009>
- DeGrassi G, Nie J, Hofmayer C (2008) Seismic analysis of large-scale piping systems for the JNES-NUPEC ultimate strength piping test program. Report No. NUREG/CR-6983, Upton, New York, <https://www.nrc.gov/reading-rm/doc-collections/nuregs/contract/cr6983/>
- Di Sarno L, Karagiannakis G (2019) Petrochemical steel pipe rack: critical assessment of existing design code provisions and a case study. *Int J Steel Struct*. <https://doi.org/10.1007/s13296-019-00280-w>
- Elnashai AS, Di Sarno L (2015) Fundamentals of earthquake engineering: from source to fragility
- EN 1998–3 (2004) EN 1998–3. Assessment and retrofitting of buildings
- EU (2018) EU-U.S. Joint Statement of 25 July: European Union imports of U.S. Liquefied Natural Gas (LNG) are on the rise. European Commission, press release database, https://ec.europa.eu/commission/presscorner/detail/en/IP_18_4920#_ftn1

- Fardis MN (2014) Perspectives on European Earthquake Engineering and Seismology: Volume 1. A. Ansal, ed., Springer International Publishing, 227–266, https://doi.org/10.1007/978-3-319-07118-3_7
- Firoozabad ES, Jeon BG, Choi HS, Kim NS (2015) Seismic fragility analysis of seismically isolated nuclear power plants piping system. *Nucl Eng Des* 284:264–279
- Fouquiau P, Barbier F, Chatzigogos C (2018) New Dynamic Decoupling Criteria for Secondary Systems. In: 16th European conference on earthquake engineering, Thessaloniki, Greece, 1–10
- Jalayer F, Cornell CA (2009) Alternative nonlinear demand estimation methods for probability based seismic assessments. *Earthq Eng Struct Dyn* 38:951–972. <https://doi.org/10.1002/eqe.876>
- Karamanos SA (2016) Mechanical behavior of steel pipe bends: an overview. *J Press Vessel Technol Trans ASME* 138(4):041203. <https://doi.org/10.1115/1.4031940>
- Kothari P, Parulekar YM, Reddy GR, Gopalakrishnan N (2017) In-structure response spectra considering nonlinearity of RCC structures: Experiments and analysis. *Nucl Eng Des* 322:379–396. <https://doi.org/10.1016/j.nucengdes.2017.07.009>
- Krausmann E, Cruz AM, Affeltranger B (2009) The impact of the 12 May 2008 Wenchuan earthquake on industrial facilities. *J Loss Prev Process Ind* 2:242–248. <https://doi.org/10.1016/j.jlp.2009.10.004>
- Lanzano G, Santucci de Magistris F, Fabbrocino G, Salzano E (2015) Seismic damage to pipelines in the framework of Na-Tech risk assessment. *J Loss Prev Process Ind* 33:159–172. <https://doi.org/10.1016/j.jlp.2014.12.006>
- Mander JB, Priestley MJN, Park R (1988) Theoretical stress-strain model for confined concrete. *J Struct Eng Am Soc Civ Eng* 114(8):1804–1826. [https://doi.org/10.1061/\(ASCE\)0733-9445\(1988\)114:8\(1804\)](https://doi.org/10.1061/(ASCE)0733-9445(1988)114:8(1804))
- Margaris BN, Hatzidimitriou PM (2002) Source spectral scaling and stress release estimates using strong-motion records in Greece. *Bull Seismol Soc Am* 92(3):1040–1059
- Menegotto M, Pinto PE (1973) Method of analysis for cyclically loaded R. C. plane frames including changes in geometry and non-elastic behavior of elements under combined normal force and bending. In: Proceedings of IABSE symposium on resistance and ultimate deformability of structures acted on by well defined loads, 15–22
- Midas GEN (v2.1) (2018) MIDAS information technologies Co., Ltd. <https://en.midasuser.com/>
- Paolacci F, Bursi OS (2014) Seismic design criteria of refinery piping systems. *Greek Journal Metallikes Kataskeves*
- Paolacci F, Corritore D, Caputo AC, Bursi OS, Kalemli B (2018) A probabilistic approach for the assessment of LOC events in steel storage tanks under seismic loading. *American Society of Mechanical Engineers, Pressure Vessels and Piping Division (Publication) PVP*, 8, <https://doi.org/10.1115/PVP2018-84374>
- Paolacci F, Phan HN, Corritore D, Alessandri S, Bursi OS, Reza MS (2015) Seismic fragility analysis of liquid storage tanks. In: 5th ECCOMAS thematic conference on computational methods in structural dynamics and earthquake engineering
- Papadrakakis M, Karamanos SA, Papageorgiou AS, Karakostas C (2015) Risk assessment for the seismic protection of industrial facilities. <https://rasor.ntua.gr/>
- Papageorgiou AS (2003) The barrier model and strong ground motion. *Pure Appl Geophys* 160(3):603–634. https://doi.org/10.1007/978-3-0348-8010-7_9
- Park H-S, Lee T-H (2015) Seismic performance evaluation of boil-off gas compressor in LNG terminal. *Open Civ Eng J* 9(1):557–569
- Pitilakis K, Argyroudis S, Kaynia AM, Johansson J (2011) Systemic seismic vulnerability and risk analysis for buildings, lifeline networks and infrastructures safety gain. 1–59, <https://www.vce.at/SYNER-G/index.htm>
- Salem YS, Tiffany YPE, Gad GM, Cho JS (2019) Analytical fragility curves for pipe rack structure. *Adv Chall Struct Eng* 292–306
- Seismosoft (2016) *SeismoStruct 2016*—a computer program for static and dynamic nonlinear analysis of framed structures. <https://www.seismosoft.com>
- Straub D, Der Kiureghian A (2008) Improved seismic fragility modeling from empirical data. *Struct Saf* 30(4):320–336. <https://doi.org/10.1016/j.strusafe.2007.05.004>
- Taghavi S, Miranda E (2008) Effect of interaction between primary and secondary systems on floor response spectra. In: 14th world conference on earthquake engineering, Beijing, China, 12–17
- Tsionis G, Argyroudis S, Babič A, Billmaier M, Dolšek M, Esposito S, Giardini D, Iervolino I, Iqbal S, Krausmann E, Matos JP, Mignan A, Pitilakis K, Salzano E, Schleiss AJ, Selva J, Stojadinović B, Zwicky P (2016) The STREST project: Harmonized approach to stress tests for critical infrastructures against low-probability high-impact natural hazards. In: Proceedings of the 6th international disaster and risk conference: integrative risk management—towards resilient cities, IDRC Davos 2016, 598–601

- Tsionis G, Fardis M (2014) Seismic fragility curves for reinforced concrete buildings and bridges in Thessaloniki. In: Second European conference on earthquake engineering and seismology. <https://publications.jrc.ec.europa.eu/repository/handle/JRC90016>
- Vamvatsikos D, Cornell CA (2004) Applied incremental dynamic analysis. *Earthq Spectra* 20(2):523–553
- Vathi M, Karamanos SA, Kapogiannis IA, Spiliopoulos KV (2017) Performance criteria for liquid storage tanks and piping systems subjected to seismic loading. *J Press Vessel Technol Trans ASME*. <https://doi.org/10.1115/1.4036916>
- Young S, Balluz L, Malilay J (2004) Natural and technologic hazardous material releases during and after natural disasters: a review. *Sci Total Environ* 322(1–3):3–20. [https://doi.org/10.1016/S0048-9697\(03\)00446-7](https://doi.org/10.1016/S0048-9697(03)00446-7)

Publisher's Note Springer Nature remains neutral with regard to jurisdictional claims in published maps and institutional affiliations.